New Journal of Physics
The open access journal for physics

Two-dimensional vibronic spectroscopy of molecular predissociation

Julian Albert, Alexander Schubert and Volker Engel[1]
Universität Würzburg, Institut für Physikalische und Theoretische Chemie and Röntgen Research Center for Complex Material Systems, Hubland Campus Nord, Emil-Fischer-Straße 42, D-97074 Würzburg, Germany
E-mail: voen@phys-chemie.uni-wuerzburg.de

New Journal of Physics **15** (2013) 025008 (13pp)
Received 12 October 2012
Published 5 February 2013
Online at http://www.njp.org/
doi:10.1088/1367-2630/15/2/025008

Abstract. We calculate two-dimensional (2D) spectra reflecting the time-dependent electronic predissociation of a diatomic molecule. The laser-excited electronic state is coupled non-adiabatically to a fragment channel, leading to the decay of the prepared quasi-bound states. This decay can be monitored by the three-pulse configuration employed in optical 2D spectroscopy. It is shown that in this way it is possible to state-selectively characterize the time-dependent population of resonance states with different lifetimes. A model of the NaI molecule serves as a numerical example.

Contents

[1] Author to whom any correspondence should be addressed.

1. Introduction

In 1988, Zewail and co-workers performed the first femtosecond time-resolved spectroscopic study of a molecular predissociation process [1–3]. In these experiments, the electronic excitation of NaI molecules initiates a quasi-bound wave-packet motion. The excited state—which is non-adiabatically coupled to a dissociation continuum—falls apart and the decay (or, alternatively, the production of fragments) was monitored by pump–probe fluorescence spectroscopy. This important decay dynamics has been studied extensively both experimentally [4–10] and theoretically [11–20].

In another key experiment on NaI which was also performed in the Zewail group [21], it was shown that the long-time transient signals exhibit the so-called 'revival' structures [22], which are well known from experiments on atomic and molecular bound-state systems [23–30]. In the case of NaI, these features are related to the excitation of long-lived resonance states which have been characterized theoretically using semiclassical mechanics [31]. In the latter study, it was shown that the system possesses resonances with lifetimes which vary periodically as a function of energy. As a consequence, the wave packet initially prepared by the femtosecond pump pulse decays into the fragment channel where components belonging to short-lived states enter first, whereas the components belonging to the long-lived resonances decay later, a behavior that has been documented theoretically [32]. In this work, we propose to use two-dimensional (2D) optical spectroscopy to monitor such a predissociation dynamics.

2D spectroscopy, which is a standard technique in nuclear magnetic resonance experiments [33, 34], is now also frequently used in the infrared region [35–37]. The technique was extended to light sources acting in the optical regime [38–42] and more and more applications have appeared in recent years [43–50]. Although the potential of optical 2D spectroscopy lies in the analysis of coupled systems in dissipative environments, it is also possible to apply this technique to gas-phase systems [51–53] where coherence is not destroyed by system–bath interactions. This situation can then be described theoretically using a wave-function approach [54–56] instead of adopting the powerful description in terms of the density-matrix formalism [57–67].

In what follows, we present wave-packet calculations on the gas-phase 2D spectroscopy of a predissociation process. In section 2 we summarize the details of the model and the calculation of the 2D spectra. Numerical results are presented in section 3, which also contains a short conclusion.

2. Theory

2.1. The model

For our numerical simulations, we use potential energy curves of two electronic states of the NaI molecule [68, 69], which are displayed in figure 1. Shown are diabatic curves $V_n^{\mathrm{d}}(R)$ which cross at a distance of about 7 Å and also adiabatic potentials $V_n^{\mathrm{a}}(R)$ which show an avoided crossing. The diabatic bound state $|0\rangle$ (which is ionic in character) and the excited dissociative state $|1\rangle$ (being covalent in character) interact via a coupling element $V_{\mathrm{c}}(R)$ [12]. Neglecting rotations, the molecular Hamiltonian is

$$H_0 = \sum_{n=0}^{1} |n\rangle (T_R + V_n^{\mathrm{d}}(R)) \langle n| + |0\rangle V_{\mathrm{c}}(R) \langle 1| + |1\rangle V_{\mathrm{c}}(R) \langle 0|, \tag{1}$$

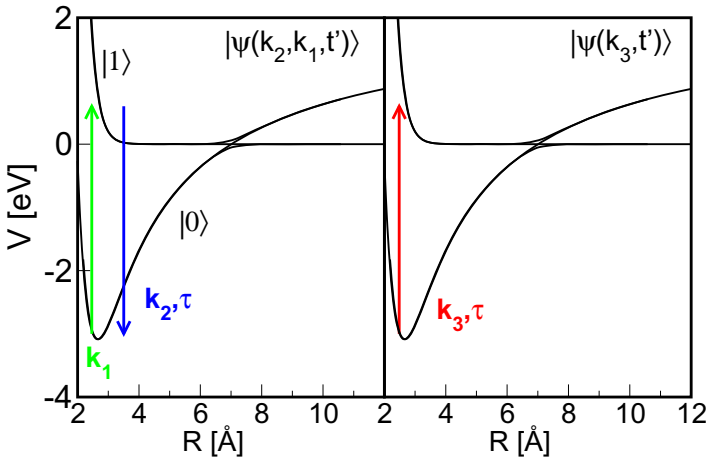

Figure 1. Potential energy curves of the NaI molecule: shown are diabatic curves which cross at a distance of about 7 Å and also the adiabatic curves which exhibit an avoided crossing. Excitation by a femtosecond pulse ($\mathbf{k}_1$) leads to a predissociative wave-packet motion. The decay dynamics is monitored by the interaction with time-delayed laser pulses ($\mathbf{k}_2$, $\mathbf{k}_3$) which interact simultaneously at time τ. The left-hand panel illustrates the preparation of the second-order state $|\psi^{(2)}(\mathbf{k}_2, \mathbf{k}_1, t')\rangle$ and the right-hand panel that of the first-order state $|\psi^{(1)}(\mathbf{k}_3, t')\rangle$. These states determine the third-order time-dependent polarization (equation (6)).

where T_R denotes the kinetic energy operator. In order to facilitate the numerical calculations, we first work with a reduced mass that is a factor of 5 smaller than that of the NaI molecule. This has the consequence that the vibrational period of the quasi-bound motion at an excitation energy of 3.6 eV is $T_{\mathrm{vib}} \approx 0.4$ ps, as compared to ≈ 1 ps in NaI.

The interaction of three ultrashort laser pulses which is relevant for 2D spectroscopic measurements is taken within the rotating-wave approximations as

$$W(t) = -\left[|1\rangle\mu E^{(+)}(t)\langle 0| + |0\rangle\mu E^{(-)}(t)\langle 1|\right], \tag{2}$$

with the projection μ of the transition dipole moment on the laser polarization vector. This projection is taken to be constant and the same for all pulses. Because all radiative transitions take place in the vicinity of the ground-state equilibrium position, this approximation (Condon approximation) is valid. The fields that induce an absorption (+) or emission (−) process are defined as

$$\begin{aligned} E^{(\pm)}(t) &= \sum_{n=1}^{3} E_n^{(\pm)}(t) \\ &= \frac{1}{2}\sum_{n=1}^{3} g_n(t-T_n)\, \mathrm{e}^{\mathrm{i}[\mp\omega_n(t-T_n)\pm\mathbf{k}_n\mathbf{x}]} \end{aligned} \tag{3}$$

and are characterized by their frequencies ω_n, wave vectors ($\mathbf{k}_n$) and pulse envelopes $g_n(t-T_n)$. The times T_n denote the center of the envelope functions. We use a pulse configuration where a first pulse ($\mathbf{k}_1$) interacts at time $T_1 = 0$, whereas pulses ($\mathbf{k}_2$, $\mathbf{k}_3$) act simultaneously at the delay

time $\tau = T_2 = T_3$. All pulse envelopes are Gaussians with a width (full-width at half-maximum) of 30 fs and possess the same photon energy of $\hbar\omega = 3.6\,\mathrm{eV}$.

The initial state of our calculations is the vibrational ground state $\psi_0(R)$ in $|0\rangle$ and wave functions that enter the spectra are determined within the dipole approximation and time-dependent perturbation theory [70, 71]. The propagation is performed with the split-operator technique [72]. We use a grid ranging from $R = 1$ to 20 Å with 1024 grid points. The time step for the propagation is 0.5 fs. The outgoing wave packets in the dissociation channel are smoothly removed by a cut-off function of the form

$$f(R) = \begin{cases} 1.0 & (R \leqslant R_c), \\ \cos^2\left[(R - R_c)\pi/L\right] & (R > R_c). \end{cases} \tag{4}$$

The parameters $R_c = 15$ Å and $L = 10$ Å are chosen such that $f(R)$ vanishes at the end of the numerical grid.

2.2. Two-dimensional spectra

The 2D spectra are calculated from the third-order time-dependent polarization [73]

$$P^{(3)}(t, \tau) = \sum_{m=0}^{3} \langle \psi^{(m)}(t) | \mu | \psi^{(3-m)}(t) \rangle, \tag{5}$$

with wave functions $|\psi^{(j)}\rangle$ determined from time-dependent perturbation theory of order (j). In a typical 2D experiment, the detection direction selects only those terms where the field wave vectors fulfill the equation $\mathbf{k}_s = -\mathbf{k}_1 + \mathbf{k}_2 + \mathbf{k}_3$. In what follows, we regard only times when the pulse $(\mathbf{k}_1)$ does not overlap with the pulses $(\mathbf{k}_2, \mathbf{k}_3)$. It can then be shown that from all the terms appearing in equation (5) only two remain that are identical [56] and we have

$$P_T^{(3)}(t', \tau) = 2\,\langle \psi^{(2)}(\mathbf{k}_2, \mathbf{k}_1, t') | \mu | \psi^{(1)}(\mathbf{k}_3, t') \rangle. \tag{6}$$

Here, a new time variable t' enters which is measured with respect to the delay time τ. The polarization is now determined for several equidistant values of the delay time τ in an interval starting at time T, as indicated by the subscript in equation (6).

The second-order state $|\psi^{(2)}(\mathbf{k}_2, \mathbf{k}_1, t')\rangle$ appearing in the last equation results from two interactions: an excited-state wave packet is prepared by the first laser pulse, and this packet is dumped down to the ground state by pulse $(\mathbf{k}_2)$ at the delay time τ, see figure 1. The polarization is determined by the overlap of this state with the first-order state $|\psi(\mathbf{k}_3, t')\rangle$ that results from absorption of a photon from pulse $(\mathbf{k}_3)$ at time τ.

For the purpose of illustration, we regard the case of two field-coupled bound molecular states in the impulsive limit where all three pulses are taken as δ-functions in time (note, however, that the numerical calculation involves Gaussian pulses of 30 fs width). In this case, the polarization can be written as [56]

$$P_T^{(3)}(t', \tau) \sim \sum_{n_1} \sum_{n_0} \sum_{m_1} a(i_0, n_1, n_0, m_1) \mathrm{e}^{\mathrm{i}(E_{n_1} - E_{i_0})\tau/\hbar}\, \mathrm{e}^{\mathrm{i}(E_{n_0} - E_{m_1})t'/\hbar} \Theta(\tau - T). \tag{7}$$

Here, E_{i_0} is the energy of the initial state and the ground (excited) state vibrational energies are denoted by E_{n_0} (E_{n_1}, E_{m_1}), respectively. The coefficients $a(i_0, n_1, n_0, m_1)$ contain dipole matrix elements between the ground- and excited-state vibrational wave functions, and the

Heaviside Θ-function is introduced to mark the origin of the time interval for the delay time τ. Thus, the polarization contains coherences between the excited and ground-state energies of the system. In the present case, the excited state is predissociative and no bound states exist. Phenomenologically, we may adopt equation (7) in replacing the energy levels (E_{k_1}) by ($E_{k_1} - \mathrm{i}\hbar\gamma_k/2$), where γ_k denotes the inverse lifetime of the resonance state with energy E_{k_1}:

$$P_T^{(3)}(t', \tau) \sim \sum_{n_1} \sum_{n_0} \sum_{m_1} a(i_0, n_1, n_0, m_1) \mathrm{e}^{\mathrm{i}(E_{n_1} - E_{i_0})\tau/\hbar}\, \mathrm{e}^{\mathrm{i}(E_{n_0} - E_{m_1})t'/\hbar} \mathrm{e}^{-\gamma_{n_1}\tau/2}\, \mathrm{e}^{-\gamma_{m_1}t'/2}\, \Theta(\tau - T). \tag{8}$$

The particular values of the lifetimes will determine the appearance of the 2D spectrum as discussed below.

The 2D spectrum itself is obtained by Fourier transformation [64] as

$$S_T(E_{t'}, E_\tau) = \mathrm{i} \int \mathrm{d}\tau \int \mathrm{d}t'\, \mathrm{e}^{\frac{\mathrm{i}}{\hbar}(E_{t'}t' - E_\tau\tau)}\, P_T^{(3)}(t', \tau). \tag{9}$$

From the expression for the polarization (equation (7)) it is then obvious that along the energy axis $E_{t'}$, peaks appear which correspond to differences between excited and ground-state levels, whereas along the E_τ-axis the peak positions occur at differences between excited-state levels and the vibronic ground state, i.e. the initial state of the system. In the here treated situation, the excited states are resonance states but it will be shown that a 'vibrational' structure can still be seen in the spectra but critically depends on the sampling interval for the delay time τ.

3. Results

We first study the predissociation for a model system where the potential curves of NaI are employed but the molecular mass is reduced by a factor of 5. As is mentioned in the introduction, the absorption spectrum consists of a progression of lines, which correspond to long- and short-lived resonance states. This is documented in figure 2, which shows the spectrum calculated as the Fourier transform of the autocorrelation function [74, 75]

$$\sigma_{\mathrm{abs}}(E) = \int \mathrm{d}t\, \mathrm{e}^{\mathrm{i}Et} \langle \mu\psi_0 | \mathrm{e}^{-\mathrm{i}H_0 t} \mu\psi_0 \rangle\, w(t), \tag{10}$$

with the vibronic ground-state wave function ψ_0. Spectra are determined for different window functions defined as

$$w(t) = \begin{cases} \cos^2\left[(t\pi)/(2t_w)\right] & (|t| \leqslant t_w) \\ 0 & (|t| > t_w). \end{cases} \tag{11}$$

The times t_w, which are indicated in the panel of figure 2, determine the spectral resolution. Many lines can be seen in the spectra. In going from the low-resolution (at $t_w = 1$ ps) to the high-resolution spectrum (at $t_w = 14$ ps), groups of resonances with different lifetimes can be distinguished where the low-/high-intensity peaks correspond to short-/long-lived states.

We now turn to the 2D spectra. They are calculated via the Fourier transform of the time-dependent polarization (equation (6)). The latter is determined for discrete times t'_n taken in the interval $[\tau, \tau + t_{\max}]$, with $t_{\max} = 2.4$ ps. Likewise, the interval for the second time-variable τ_n is chosen as $[T, T + t_{\max}]$. The number of equidistant sampling points is $N_s = 4800$ in each direction. Because we are interested in the relative decay of resonance states with different lifetimes, all spectra shown are normalized to the most intense line.

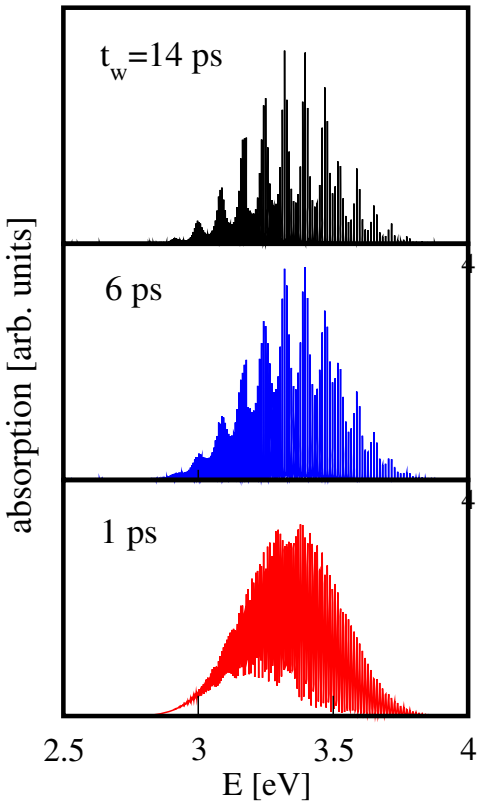

Figure 2. Absorption spectra for the predissociation model (a factor of 5 smaller mass of NaI). Spectra are shown for different resolutions as characterized by the times t_w which enter the calculation of the spectra (equation (10)).

Let us first discuss the case where we close the predissociation channel and take the excited-state potential as the adiabatic bound-state potential $V_1^a(R)$. Then, the laser pulses couple the ground- and excited-state vibrational states, which leads to the carpet-like structure seen in figure 3 (upper panel). There, we show the spectrum only in a limited region of energy space. The intensity of the single peaks depends on the Franck–Condon factors, on the one hand, and on the spectral distribution of the laser pulses, on the other. As motivated in section 2.2, each peak belongs to a difference between the excited and ground-state vibrational energies. If the coupling to the dissociation channel is included and the initial sampling time is chosen as $T = 0$ fs, the spectrum contains information about the short-time evolution of the system. We note that, for $T = 0$, there is an overlap of the three laser pulses which was excluded in the considerations presented in section 2.2. This, however, is unsubstantial for the numerical results which are not altered if $T = 0$ is changed to a time of $T = 100$ fs, where no overlap exists.

Figure 3 (lower panel) shows the spectrum obtained if the non-adiabatic coupling is included. If compared to the 'adiabatic' case (upper panel), it is seen that the two spectra are very similar. This is due to the fact that the non-adiabatic coupling is rather small so that, at early times, the fragmentation channel is only weakly populated and, to a first approximation, the dynamics proceeds adiabatically in the upper bound-state potential.

In figure 4, we show 2D spectra calculated for times $T = 1$, 2 and 6 ps, respectively. In increasing the sampling origin T, we probe the dynamics in the delay-time variable at later and

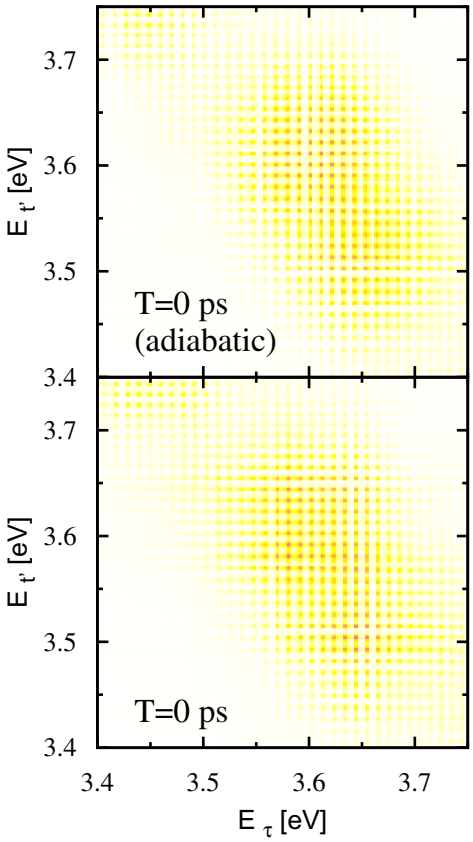

Figure 3. Modulus of 2D spectra at $T = 0$. Upper panel: the predissociation channel is not included in the calculation (adiabatic motion). Lower panel: spectrum from a calculation where the coupling to the dissociation channel is taken into account. The sampling interval for the delay time covers times from 0 to 2.4 ps (short-time dynamics).

later times. This can be seen from the expression for the polarization equation (8). For states with a lifetime which is much shorter than the sampling origin T, the exponential factor $e^{-\gamma_{n_1}\tau/2}$ damps out the corresponding term in the sum so that it no longer appears. States with a much longer lifetime, however, contribute to the spectrum. Accordingly, the 2D spectrum will exhibit intensity only at energy differences where the energies of resonance states that possess much longer lifetimes enter. Note that this is not necessarily true along the $E_{t'}$-direction. The levels with quantum numbers m_1 are populated by the $\mathbf{k}_3$-interaction initiating in the ground-state. Their time dependence (carrying an exponential damping with the factor $e^{-\gamma_{m_1}t'/2}$) is probed only for the sampling length $t_{\max}$, i.e. the short-time dynamics is probed. On the other hand, the ground-state levels with energies E_{n_0} are populated by stimulated emission by the pulse ($\mathbf{k}_2$), originating from the moving wave packet in the upper state which has already evolved in time until τ. Thus the transitions occur only from still populated levels. Obviously, there are so many energy differences between the excited and ground-state vibrational states available so that no regions of low intensity appear along the $E_{t'}$-axis.

In comparing the 2D spectra for the three values of T, we see that at certain values of E_τ they lose intensity significantly faster. As a consequence, stripes parallel to the $E_{t'}$-axis appear

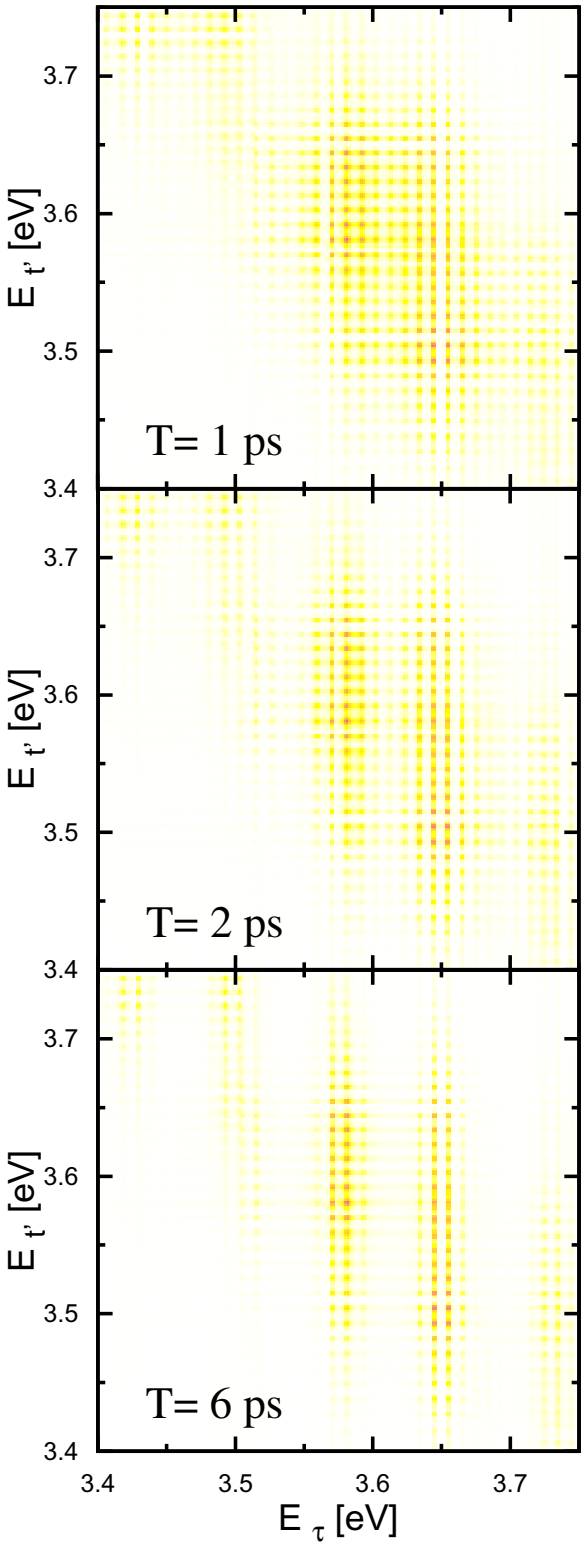

Figure 4. Modulus of the 2D spectra for different delay-time sampling origins T, as indicated. With increasing the time T, the decay of short-lived resonances leads to an intensity loss at the respective energies E_τ.

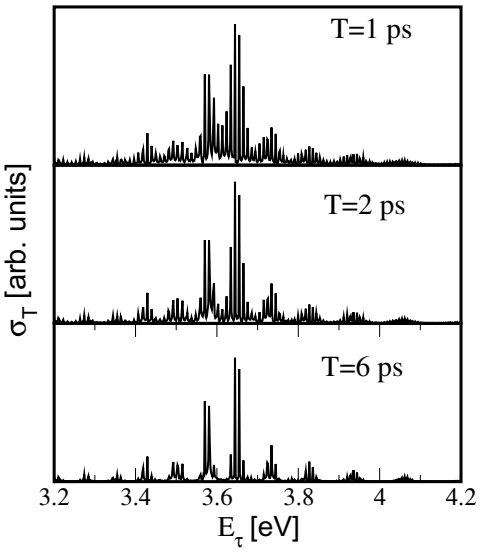

Figure 5. Integrated spectra $\sigma_T(E_\tau)$ for different delay-time sampling origins T, as indicated.

which become sharper as time goes along. This trend continues for larger values of T (not shown). From what has been said above, this means that the intensity loss corresponds to the decay of resonance states of certain energies. For example, resonances with short lifetimes occur around energies of 3.54 and 3.62 eV, see figure 4 (lower panel). This is, as expected, consistent with the features of the absorption spectrum. Although, for the laser pulse parameters employed, a different energy range is probed, the resonances are found at the same energies (figure 2). The connection becomes even clearer if we regard the energy integrated 2D spectra:

$$\sigma_T(E_\tau) = \int \mathrm{d}E_{t'} \, |S_T(E_{t'}, E_\tau)|, \tag{12}$$

which are displayed in figure 5 for the same sampling times T as regarded in figure 4.

At the shortest time $T = 1$ ps, a vibrational structure is visible but the characteristic resonance structure becomes more pronounced with increasing T. Here, the clear gaps in the spectrum at the longest time $T = 6$ ps correspond to the stripes of missing intensity in figure 4 (lower panel). The decrease of the intensity directly monitors the decay of the resonance states.

To extract resonance lifetimes, it is possible to regard single peaks of the 2D spectra and monitor the decay of the peak height as a function of the time T. In figure 6 we show this for two peaks at energies $E_\tau = E_{t'} = 3.581$ and 3.614 eV, respectively. The figure documents the different decay behaviors. For the shown curves we used a fixed energy in each case and numerical fluctuations are seen. In order to obtain accurate decay rates, the spectra should be integrated over energy to eliminate fluctuation.

Let us now regard the NaI system, taking the correct molecular mass into account. This leads to a much larger density of resonance- and ground-state levels. To show that the behavior here is no different from the one illustrated in the example given above, we calculate low-resolution spectra. Therefore, the sampling intervals are chosen to have a length of 0.512 ps. This means that the quasi-bound motion in the excited state is probed for only about half a vibrational period, so that no vibrational sub-structure is to be expected. In figure 7 we compare spectra for

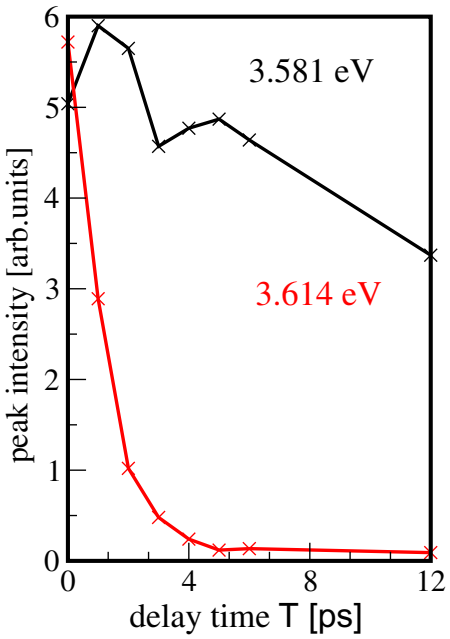

Figure 6. Decay of resonance peaks at two (diagonal, $E_\tau = E_{t'}$) energies, as indicated. The resonance corresponding to the energy of 3.581 eV decays on a much slower time scale than the short living state at 3.614 eV.

the initial sampling times of $T = 0$ and 6 ps. At the earlier time, a structureless spectrum is found which mainly reflects the smoothed-out Franck–Condon distribution. This resembles the case where the upper state is purely dissociative [76]. Increasing the time to $T = 6$ ps, we again find the characteristic stripes parallel to the $E_{t'}$-axis which tell us that resonance states of particular energies already decayed whereas others are longer lived.

To conclude, we demonstrate the power of 2D-vibronic spectroscopy in monitoring predissociation processes by performing time-dependent quantum calculations. It is seen that spectra determined for delay times sampled at early times differ from those obtained at later times. In particular, the decay of resonances with different resonance energies and lifetimes can be mapped state selectively and decay rates can be obtained from the 2D spectra. In our numerical example, the particular resonance structure of the NaI molecule is revealed where the lifetimes of quasi-bound states vary periodically as a function of energy (figure 7).

Let us finally comment on the detection of the resonance decay by other measurements. The evidence for the existence of long- and short-lived resonances was already deduced from the early pump–probe fluorescence experiments by Zewail and co-workers [21]. In the latter work, however, because of the spectrally broad pulses, groups of resonances are excited so that only an average lifetime can be inferred. As another technique, one may consider transient absorption measurements. Because in these experiments ground- and excited-state levels are as well coherently coupled, the technique should also be able to detect the state-selective decay. As for energy-resolved experiments, an absorption spectrum, if recorded with sufficient resolution (such spectra were taken for NaI [77–79]), exhibits the line shapes of the single resonances and the lifetimes could, by a proper analysis, be extracted. The appealing thing of vibronic

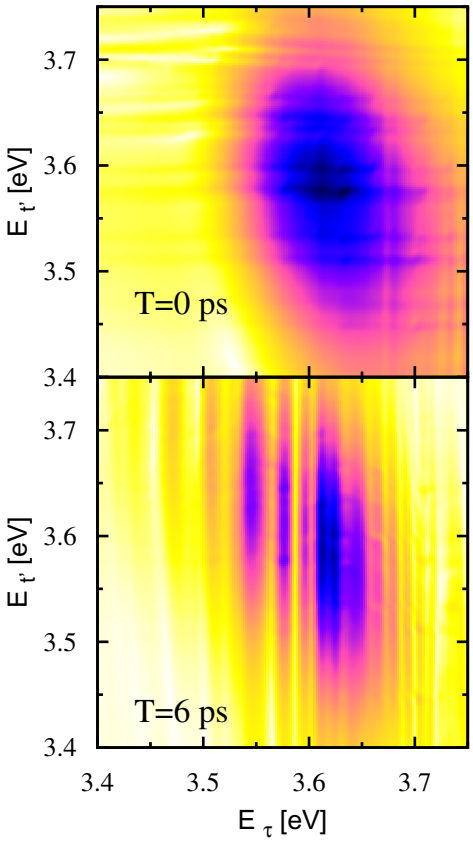

Figure 7. Modulus of 2D spectra of NaI for two sampling times T, as indicated. The spectrum at early times resembles the one of a purely dissociative state. For longer times, the resonance structure of the quasi-bound system is visible.

2D spectroscopy is, of course, the picture of a decay recorded simultaneously in the time and energy domains.

Acknowledgments

This work was funded by the German Research Foundation (DFG) within GRK 1221 and FOR 1809 and by the University of Würzburg under the funding program Open Access Publishing.

References

[1] Rose T S, Rosker M J and Zewail A H 1988 *J. Chem. Phys.* **88** 6672
[2] Rosker M J, Rose T S and Zewail A H 1988 *Chem. Phys. Lett.* **146** 175
[3] Engel V, Metiu H, Almeida R, Marcus R A and Zewail A H 1988 *Chem. Phys. Lett.* **152** 1
[4] Mokhtari A, Cong P, Herek J L and Zewail A H 1990 *Nature* **348** 225
[5] Rose T S, Rosker M J and Zewail A H 1991 *J. Chem. Phys.* **91** 7415
[6] Materny A, Herek J L, Cong P and Zewail A H 1994 *J. Phys. Chem.* **98** 3352
[7] Herek J, Materny A and Zewail A H 1994 *Chem. Phys. Lett.* **228** 15
[8] Jouvet C *et al* 1997 *J. Phys. Chem.* A **101** 2555

[9] Knopp G, Schmitt M, Materny A and Kiefer W 1997 *J. Phys. Chem.* A **101** 4852
[10] Bardeen C J, Che J, Wilson K R, Yakovlevi V V, Cong P, Kohler B, Krause J L and Messina M 1997 *J. Phys. Chem.* A **101** 3815
[11] Choi S E and Light J C 1989 *J. Chem. Phys.* **90** 2593
[12] Engel V and Metiu H 1990 *J. Chem. Phys.* **90** 6116
[13] Kono H and Fujimura Y 1991 *Chem. Phys. Lett.* **184** 497
[14] Taneichi T, Kobayashi T, Ohtsuki Y and Fujimura Y 1994 *Chem. Phys. Lett.* **231** 50
[15] Braun M, Meier C and Engel V 1996 *J. Chem. Phys.* **105** 530
[16] Grønager M and Henriksen N E 1998 *J. Chem. Phys.* **109** 4335
[17] Charron E and Giusti-Suzor A 1998 *J. Chem. Phys.* **108** 3922
[18] Hoki K, Ohtsuki Y, Kono H and Fujimura Y 1999 *J. Phys. Chem.* **103** 6301
[19] Marquetand P, Materny A, Henriksen N E and Engel V 2004 *J. Chem. Phys.* **120** 5871
[20] Marquetand P and Engel V 2005 *Phys. Chem. Chem. Phys.* **7** 469
[21] Cong P, Mokhtari A and Zewail A H 1990 *Chem. Phys. Lett.* **172** 109
[22] Robinett R W 2004 *Phys. Rep.* **392** 1
[23] Bowman R M, Dantus M and Zewail A H 1989 *Chem. Phys. Lett.* **161** 297
[24] Yeazell J A, Mallalieu M and Stroud C R 1990 *Phys. Rev. Lett.* **64** 2007
[25] Gruebele M and Zewail A H 1993 *J. Chem. Phys.* **98** 883
[26] Baumert T, Engel V, Röttermann C, Strunz W T and Gerber G 1992 *Chem. Phys. Lett.* **191** 639
[27] Fischer I, Villeneuve D M, Vrakking M J J and Stolow A 1995 *J. Chem. Phys.* **102** 5566
[28] Vrakking M J J, Villeneuve D M and Stolow A 1996 *Phys. Rev.* A **54** R37
[29] Katsuki H, Chiba H, Meier C, Girard B and Ohmori K 2009 *Phys. Rev. Lett.* **102** 103602
[30] Katsuki H, Chiba H, Girard B, Meier C and Ohmori K 2006 *Science* **311** 1589
[31] Chapman S and Child M S 1991 *J. Phys. Chem.* **95** 578
[32] Meier C, Engel V and Briggs J S 1991 *J. Chem. Phys.* **95** 7337
[33] Aue W P, Bartholdi E and Ernst R R 1976 *J. Chem. Phys.* **64** 2229
[34] Ernst R R, Bodenhausen G and Wokaun A 1987 *Principles of Nuclear Magnetic Resonance in One and Two Dimensions* (Oxford: Clarendon)
[35] Hamm P, Lim M and Hochstrasser R M 1998 *J. Phys. Chem.* B **102** 6123
[36] Khalil M, Demirdöven N and Tokmakoff A 2003 *J. Phys. Chem.* A **107** 5258
[37] Bredenbeck J, Helbing J, Kolano C and Hamm P 2007 *Chem. Phys. Chem.* **8** 1747
[38] Hybl J D, Albrecht A W, Faeder S M G and Jonas D M 1998 *Chem. Phys. Lett.* **297** 307
[39] Tian P, Keusters D, Suzaki Y and Warren W S 2003 *Science* **300** 1553
[40] Cowan M L, Ogilvie J P and Miller R J D 2004 *Chem. Phys. Lett.* **386** 184
[41] Brixner T, Mancal T, Stiopkin I and Fleming G R 2004 *J. Chem. Phys.* **121** 4221
[42] Brixner T, Stenger J, Vaswani H M, Cho M, Blankenship R E and Fleming G R 2005 *Nature* **434** 625
[43] Szöcs V, Palszegi T, Lukes V, Sperling J, Milota F, Jakubetz W and Kauffmann H F 2006 *J. Chem. Phys.* **124** 124511
[44] Engel G S, Calhoun T R, Read E L, Ahn T-K, Mancal T, Cheng Y-C, Blankenship R E and Fleming G R 2007 *Nature* **446** 782
[45] Nemeth A, Milota F, Mancal T, Lukes V, Kauffmann H F and Sperling J 2008 *Chem. Phys. Lett.* **459** 94
[46] Read E L, Schlau-Cohen G S, Engel G S, Wen J, Blankenship R E and Fleming G R 2008 *Biophys. J.* **95** 847
[47] Myers J A, Lewis K L M, Fuller F D, Tekavec P F, Yocum C F and Ogilvie J P 2010 *J. Phys. Chem. Lett.* **1** 2774
[48] Kullmann M, Ruetzel S, Buback J, Nuernberger P and Brixner T 2011 *J. Am. Chem. Soc.* **133** 13074
[49] Bixner O *et al* 2012 *J. Chem. Phys.* **136** 204503
[50] Mancal T, Christensson N, Lukes V, Milota F, Bixner O, Kauffmann H F and Hauer J 2012 *J. Phys. Chem. Lett.* **3** 1497
[51] Vaughan J C, Hornung T, Stone K W and Nelson K A 2007 *J. Phys. Chem.* A **111** 4873

[52] Dai X, Bristow A D, Karaiskaj D and Cundiff S T 2010 *Phys. Rev.* A **82** 052503
[53] Dai X, Richter M, Li H, Bristow A D, Falvo C, Mukamel S and Cundiff S T 2012 *Phys. Rev. Lett.* **108** 193201
[54] Seibt J, Renziehausen K, Voronine D V and Engel V 2009 *J. Chem. Phys.* **130** 134318
[55] Schubert A, Renziehausen K and Engel V 2010 *Phys. Rev.* A **82** 013419
[56] Schubert A and Engel V 2011 *J. Chem. Phys.* **134** 104304
[57] Zhang W M and Mukamel S 1999 *J. Chem. Phys.* **110** 5011
[58] Faeder S M G and Jonas D M 1999 *J. Phys. Chem.* A **103** 10489
[59] Mukamel S 2000 *Annu. Rev. Phys. Chem.* **51** 691
[60] Mukamel S and Abramavicius D 2004 *Chem. Rev.* **104** 2073
[61] Egorova D, Gelin M F and Domcke W 2007 *J. Chem. Phys.* **126** 074314
[62] Cho M and Fleming G R 2005 *J. Chem. Phys.* **123** 114506
[63] Cho M, Vaswani H M, Brixner T, Stenger J and Fleming G R 2005 *J. Phys. Chem.* B **109** 10542
[64] Kjellberg P, Brüggemann B and Pullerits T 2006 *Phys. Rev.* B **74** 024303
[65] Cho M 2008 *Chem. Rev.* **108** 1331
[66] Abramavicius D, Palmeiri B, Voronine D V, Sanda F and Mukamel S 2009 *Chem. Rev.* **109** 2350
[67] Gelin M F, Egorova D and Domcke W 2009 *Acc. Chem. Res.* **42** 1290
[68] Faist M B and Levine R D 1976 *J. Chem. Phys.* **64** 2953
[69] van Veen N J A, de Vries M S, Sokol J D, Baller T and de Vries A E 1981 *Chem. Phys.* **56** 81
[70] Engel V 1991 *Comput. Phys. Commun.* **63** 228
[71] Renziehausen K, Marquetand P and Engel V 2009 *J. Phys. B: At. Mol. Opt. Phys.* **42** 195402
[72] Feit M D, Fleck J A and Steiger A 1982 *J. Comput. Phys.* **47** 412
[73] Mukamel S 1995 *Principles of Nonlinear Optical Spectroscopy* (New York: Oxford University Press)
[74] Heller E J 1981 *Acc. Chem. Res.* **14** 368
[75] Schinke R 1993 *Photodissociation Dynamics* (Cambridge: Cambridge University Press)
[76] Schubert A and Engel V 2011 *Z. Phys. Chem.* **225** 703
[77] Ragone A S, Levy D H and Berry R S 1982 *J. Chem. Phys.* **77** 3784
[78] Schaefer S H, Bender D and Tiemann E 1982 *Chem. Phys. Lett.* **92** 273
[79] Schaefer S H, Bender D and Tiemann E 1984 *Chem. Phys.* **89** 65